# Unambiguous Identification of Three $\beta$-Decaying Isomers in $^{70}$Cu

J. Van Roosbroeck,[1] C. Guénaut,[2] G. Audi,[2] D. Beck,[3] K. Blaum,[3,4,*] G. Bollen,[5] J. Cederkall,[4] P. Delahaye,[4] A. De Maesschalck,[6] H. De Witte,[1] D. Fedorov,[7] V. N. Fedoseyev,[4] S. Franchoo,[4] H. O. U. Fynbo,[4,†] M. Górska,[1,3] F. Herfurth,[4] K. Heyde,[6] M. Huyse,[1] A. Kellerbauer,[4] H.-J. Kluge,[3] U. Köster,[4] K. Kruglov,[1] D. Lunney,[2] V. I. Mishin,[8] W. F. Mueller,[1] Sz. Nagy,[9] S. Schwarz,[5] L. Schweikhard,[10] N. A. Smirnova,[6] K. Van de Vel,[1] P. Van Duppen,[1] A. Van Dyck,[6] W. B. Walters,[11] L. Weissman,[1,4,‡] and C. Yazidjian[3]

[1]*IKS, University of Leuven, Celestijnenlaan 200D, 3001 Leuven, Belgium*
[2]*CSNSM-IN2P3-CNRS, 91405 Orsay-Campus, France*
[3]*GSI, Planckstraße 1, 64291 Darmstadt, Germany*
[4]*CERN, Division EP, 1211 Genève 23, Switzerland*
[5]*NSCL, Michigan State University, East Lansing, Michigan 48824-1321, USA*
[6]*Vakgroep Subatomaire en Stralingsfysica, Universiteit Gent, Proeftuinstraat 86, 9000 Gent, Belgium*
[7]*St. Petersburg Nuclear Physics Institute, 188350 Gatchina, Russia*
[8]*Institute of Spectroscopy, Russian Academy of Sciences, 142092 Troitsk, Russia*
[9]*Atomic Physics, Alba Nova, Stockholm University, 106 91 Stockholm, Sweden*
[10]*Institute of Physics, Ernst-Moritz-Arndt-University Greifswald, 17487 Greifswald, Germany*
[11]*Department of Chemistry, University of Maryland, College Park, Maryland 20742, USA*
(Received 12 November 2003; published 17 March 2004)

Using resonant laser ionization, $\beta$-decay studies, and for the first time mass measurements, three $\beta$-decaying states have been unambiguously identified in $^{70}$Cu. A mass excess of $-62\,976.1(1.6)$ keV and a half-life of 44.5(2) s for the $(6^-)$ ground state have been determined. The level energies of the $(3^-)$ isomer at 101.1(3) keV with $T_{1/2} = 33(2)$ s and the $1^+$ isomer at 242.4(3) keV with $T_{1/2} = 6.6(2)$ s are confirmed by high-precision mass measurements. The low-lying levels of $^{70}$Cu populated in the decay of $^{70}$Ni and in transfer reactions compare well with large-scale shell-model calculations, and the wave functions appear to be dominated by one proton–one neutron configurations outside the closed $Z = 28$ shell and $N = 40$ subshell. This does not apply to the $1^+$ state at 1980 keV which exhibits a particular feeding and deexcitation pattern not reproduced by the shell-model calculations.

DOI: 10.1103/PhysRevLett.92.112501 PACS numbers: 21.10.Dr, 07.75.+h, 27.50.+e, 32.80.Fb

Recent studies of the nuclear structure of $^{68}_{28}$Ni$_{40}$ aiming to establish a doubly magic character have resulted in a controversial situation where certain fingerprints for magicity such as a low-lying $0_2^+$ level, a higher-lying $2_1^+$ level, and a small $B(E2: 0_1^+ \rightarrow 2_1^+)$ are present while others are absent (see the discussion in [1]). However, some of these experimental findings can also be explained without invoking a shell closure at $N = 40$ [1]. The residual interaction between the (quasi)particle and hole states is playing a crucial role but remains poorly known. It was shown that stellar core collapse models also suffer from this lack of knowledge as these interactions influence the electron capture rates in unstable neutron-rich nuclei far from stability [2].

Crucial information to resolve this deficiency lies in the structure and $\beta$ decay of the odd-odd neighboring nuclei of $^{68}$Ni. The structure of these nuclei is particularly sensitive to the single-particle spacings between the neutron orbitals and to the specific residual interactions among the valence proton ($\pi$) and neutron ($\nu$) holes and/or particles. The single (quasi)particle components in the states of these nuclei are direct indications for the properties of $^{68}$Ni as a core nucleus. However, the specific shell-model states involved give rise to isomerism—in the case of $^{70}_{29}$Cu$_{41}$ three $\beta$-decaying isomers—which complicates significantly the study of these nuclei. The case of $^{70}$Cu is particularly interesting due to a persisting uncertainty as to the identity of the ground state.

We report a series of measurements in which resonant laser ionization has been combined with $\beta$–$\gamma$ coincidence studies and with high-resolution mass spectrometry in order to achieve the selectivity needed to elaborate the low-energy structure of $^{70}$Cu. In earlier work, two $\beta$-decaying isomers were suggested in $^{70}$Cu [3–5]; a ground state isomer with $I^\pi = (1^+)$ and $T_{1/2} = 4.5(1.0)$ s, and an isomeric state at 140(80) keV with $I^\pi = (4^-)$ and $T_{1/2} = 47(5)$ s [6]. Sherman *et al.* [7] reported five resonances from ($t$, $^3$He) studies at 0, 100(6), 226(6), 366(6), and 506(6) keV. A compilation of all prior atomic mass and decay measurements resulted in a new atomic mass evaluation of $^{70}$Cu with the ground state mass excess value of $-63\,202(15)$ keV (see [8] and references therein).

The $^{70}$Ni and $^{70}$Cu nuclei were produced in a proton-induced fission reaction on uranium. Data on the $\beta$ decay of $^{70}$Ni were obtained at the LISOL facility at Louvain-la-Neuve using the same setup as described in [9]. In-source laser spectroscopy, $\beta$-decay studies, and mass measurements of $^{70}$Cu were performed at the ISOLDE/CERN facility [10].

  

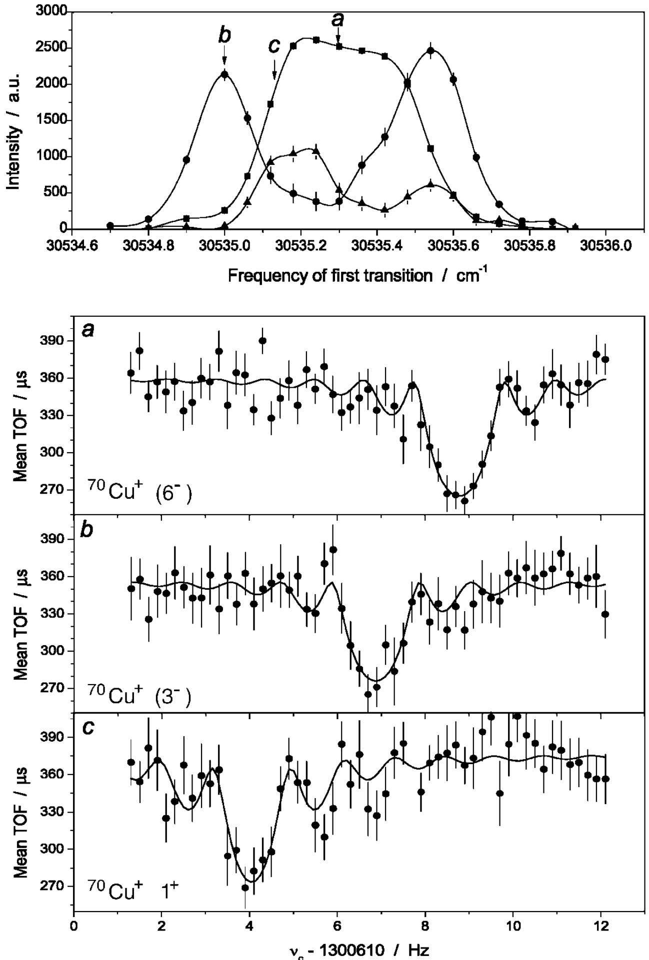


FIG. 1. Top: Intensity of the 101.1 keV (●) and 141.3 keV (▲) internal transitions summed with the associated $\beta$-delayed $\gamma$ rays as a function of laser frequency. The $\gamma$ rays associated with the decay of the $(6^-)$ ground state are indicated by (■). Bottom: Time-of-flight resonance curves as a function of cyclotron frequency for the laser settings are marked with arrows $(a, b, c)$ in the top figure. The solid lines are fits of the theoretically expected line shape to the data points.

The mass measurements on $^{70}$Cu were performed with the Penning trap mass spectrometer ISOLTRAP [11]. The setup consists of three traps. The first two traps serve for deceleration, cooling, bunching, and isobar purification of the continuous 60-keV ion beam delivered by ISOLDE. The third trap is a precision Penning trap. Here, the mass measurement is carried out by use of a time-of-flight detection technique to determine the cyclotron frequency $\nu_c = qB/(2\pi m)$ for an ion with mass $m$ and charge $q$. Cyclotron excitation times of $T_{RF} = 0.9$ s were used resulting in a linewidth $\Delta\nu_c(\mathrm{FWHM}) \approx 0.9/T_{RF} \approx 1$ Hz. This yielded a resolving power $R = \nu_c/\Delta\nu_c(\mathrm{FWHM})$ of more than $1 \times 10^6$, mandatory to clearly resolve the $^{70}$Cu isomers. The magnetic field strength $B$ was determined via the $^{85}Rb^+$ cyclotron frequency. By appropriate excitation of the ion motion, a dedicated cleaning procedure can be employed removing a possible remaining contamination from the trap. Cleaning excitation times of 3 s were used.

In the decay of $^{70}$Cu, two $\gamma$ rays from internal decay were identified with energies 101.1 and 141.3 keV. Careful scanning over the frequency of the first laser transition (Fig. 1, top) and investigation of the intensities of these two $\gamma$ lines and of the individual $\gamma$ rays in the $\beta$ decay of $^{70}$Cu revealed distinct groups of $\gamma$ rays belonging to three different hyperfine-structure patterns, evidencing the existence of three $\beta$-decaying isomers in $^{70}$Cu with spin $(6^-)$ for the lowest, $(3^-)$ for the intermediate, and $1^+$ for the highest lying isomer. Tentative spin values were deduced from the magnetic moments [12].

For the mass measurements of the three isomers, the laser frequency was tuned to the positions indicated by arrows in the upper part of Fig. 1. The obtained cyclotron resonances are shown in the lower part of Fig. 1. While for positions $a$ and $b$ the selectivity of the laser ionization was high enough to obtain almost pure samples of the $(6^-)$ and $(3^-)$ $\beta$-decaying states, in the case of position $c$ an additional mass selective cleaning of the other isomers was required to obtain an isomerically clean cyclotron resonance.

Table I gives the frequency ratios $\nu_c^{\mathrm{ref}}/\nu_c$ with respect to the reference mass $^{85}Rb^+$ for all three $^{70}$Cu states and the resulting mass excesses and literature values [8] (for details of the analysis and the residual systematic uncertainty, see [13]). The mass differences between the $\beta$-decaying states obtained with ISOLTRAP are in excellent agreement with those obtained from the decay studies of $^{70}$Ni and $^{70}$Cu and unambiguously confirm the assignments given in Fig. 2. The new mass data reveal that the literature mass excess values of all states are incorrectly evaluated by 226 keV, possibly due to a former incorrect state assignment. In addition, the new level

TABLE I. Frequency ratios relative to $^{85}Rb^+$ [$m(^{85}\mathrm{Rb}) = 84.911\,789\,732(14)$ u [8]] and mass excesses $D$ for the three $\beta$-decaying states in $^{70}$Cu as determined in this work. For comparison, literature values are given from [8]. The energies of the three isomeric states deduced from the mass measurements and the decay studies are compared.

| $^{70}$Cu | $T_{1/2}$ (s) | Frequency ratio $\nu_c^{\mathrm{ref}}/\nu_c$ | $D_{\mathrm{lit}}$ (keV) | $D_{\mathrm{exp}}$ (keV) | $E$(from mass) (keV) | $E$(from decay) (keV) |
|---|---|---|---|---|---|---|
| Ground state $(6^-)$ | 44.5(2) | 0.823 587 581 6(199) | −63 202(15) | −62 976.1(1.6) | 0 | 0 |
| First isomeric state $(3^-)$ | 33(2) | 0.823 588 854 7(258) | −63 101(16) | −62 875.4(2.0) | 100.7(2.6) | 101.1(3) |
| Second isomeric state $1^+$ | 6.6(2) | 0.823 590 641 9(272) | −62 960(16) | −62 734.1(2.1) | 242.0(2.7) | 242.4(4) |

assignments of $^{70}$Cu differ drastically from the literature values since to the new findings presented the ground state is the high-spin state with $(6^-)$ instead of $1^+$ and the second isomeric state is the low-spin state with $1^+$ instead of $(6^-)$.

These results, the decay study of $^{70}$Ni and its daughter $^{70}$Cu, and the results from the $(t, {}^3\text{He})$ reaction [7] were combined to construct the level scheme of $^{70}$Cu (see Fig. 2) and to determine both half-life and branching ratio of each $\beta$-decaying state [14]. Five $1^+$ states are populated through allowed Gamow-Teller (GT) $\beta$ decay of $^{70}$Ni and proceed to the $1^+$ isomer via one or at most two $\gamma$ transitions. Of particular interest is the unanticipated decay of the $(1^+)$ state at 1980.1 keV that is populated by an allowed $\beta$-decay branch ($\log ft = 4.5$). In contrast to all other $(1^+)$ levels, it feeds only a level at 368.9 keV and surprisingly not the $1^+$ state at 242.4 keV.

In the extreme shell-model picture, $^{70}_{29}$Cu$_{41}$ can be viewed as having one valence proton outside the $Z = 28$ closed shell and one valence neutron outside the closed $N = 40$ subshell, as shown in the left part of Fig. 2. In $^{70}$Cu, the valence proton and neutron will couple, giving rise to a multiplet of states that due to the residual interaction split up in energy [15,16]. The most important $\pi$-$\nu$-coupling schemes assuming a pure quadrupole proton-neutron interaction are schematically drawn in Fig. 2. This simplified approach serves as a guideline for the different configurations of the low-lying states observed.

The $^{70}$Cu ground state and its first excited isomeric state at 101.1 keV were already attributed to the $6^-$ and $3^-$ members of the $\pi 2p_{3/2}\nu 1g_{9/2}$ multiplet [12]. The states at 226(6) and 506(6) keV are most probably the other members [7,17]. Based on the $\gamma$ feeding and decay pattern of the states at 229 and 369 keV, we associate the latter with the $(2^-)$ member and the former to the $(4^-)$ member of the $\pi 1f_{5/2}\nu 1g_{9/2}$ multiplet. The state at 320.7 keV can be associated with the $2^+$ member of the $(1, 2)^+$ doublet having the $\pi 2p_{3/2}\nu 2p_{1/2}^{-1}$ configuration.

To further explore this configuration, we have performed large-scale shell-model calculations using a realistic effective interaction as given by $G$-matrix calculations [18] with the modified monopole part [19]. The model space consists of the $(1f_{5/2}2p_{3/2}2p_{1/2}1g_{9/2})$ orbitals outside the $^{56}$Ni core.

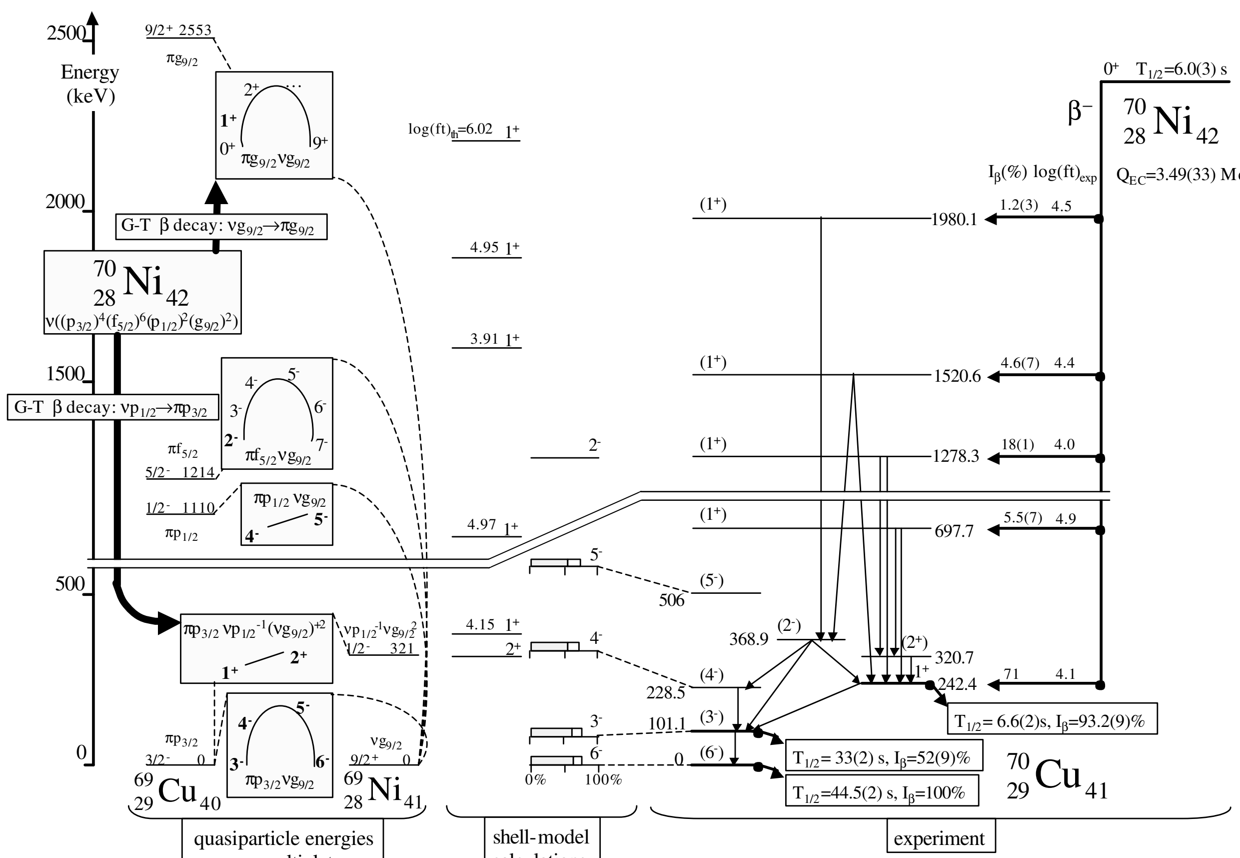


FIG. 2. Left: Schematic presentation of the experimental quasiparticle energies of the orbitals involved for $^{69}$Cu and $^{69}$Ni [6], the schematic $p$-$n$ coupling schemes, and the GT $\beta$-decay modes of $^{70}$Ni. Middle: large-scale shell-model calculations. The grey area on top of the $3^-$–$6^-$ multiplet indicates the contribution of the proposed $\pi 2p_{3/2}\nu 1g_{9/2}$ configuration, the white area indicates the $\pi 2p_{3/2}\nu(1f_{5/2}^{-2}1g_{9/2}^3)$ configurations, and the total neutron $2p$-$2h$ admixture represents 33% − 38%. Right: Partial decay scheme of $^{70}$Ni. The $(5^-)$ state is from [7].

The results of the diagonalization, performed with the shell-model code ANTOINE [20], are in good agreement with the experimental data (Fig. 2). Although the calculations show mixing between the different configurations, the contribution of the proposed $\pi 2p_{3/2}\nu 1g_{9/2}$ configuration in the first $6^-$, $3^-$, $4^-$, and $5^-$ states is more than 50% (grey area in Fig. 2), which lends support to calculations that use a more schematic force [14]. The neutron $2p$-$2h$ excitations across $N = 40$ represent in these states about 33%–38%, which is in line with the 35% admixture in the ground state of $^{68}$Ni deduced from large-scale diagonalization shell-model calculations [1].

The structure of the lowest $1^+$ and $2^+$ states is dominated by the $\pi 2p_{3/2}\nu(2p_{1/2}^{-1}1g_{9/2}^2)$ configuration, with the second largest component being $\pi 2p_{3/2}\nu(2p_{1/2}^{-1}1f_{5/2}^{-2}1g_{9/2}^4)$. All other states are predicted to have a strongly mixed wave function; none of them contain a single component contributing more than 16%.

The $1^+$ states lying within the $Q_{\mathrm{EC}}$ window will be populated in the $\beta$ decay of $^{70}$Ni through allowed GT decay leading to neutron hole states in the $2p_{1/2}$, $2p_{3/2}$, $1f_{5/2}$ orbitals or neutron particle states in the $1g_{9/2}$ orbital. Whereas the experimental $\log ft$ values for the transitions to the three lowest $1^+$ states are well reproduced by the large-scale shell-model calculations, a large deviation shows up for the $1^+$ level at 1980 keV. The particular $\gamma$-decay pattern from this $1^+$ state seems to be consistent with a dominant $\pi 1g_{9/2}\nu 1g_{9/2}$ character of the wave function for that state in an extreme shell-model picture (see Fig. 2). This suggestion, however, is not corroborated by the large-scale shell-model calculations that lead to a theoretical $\log ft$ value of 6.02 and to strong fragmentation of the $\pi 1g_{9/2}\nu 1g_{9/2}$ configuration over many states, posing a problem with respect to the precise location of the $\pi 1g_{9/2}\nu 1g_{9/2}$ centroid. These important deviations between the data and the results from present large-scale shell-model calculations clearly indicate the need to study the $\langle \pi 1g_{9/2}\nu 1g_{9/2}; J^\pi | V | \pi 1g_{9/2}\nu 1g_{9/2}; J^\pi \rangle$ two-body matrix elements for nuclei in the Ni region near mass $A = 70$ in more detail.

In conclusion, the unique combination of resonant laser ionization, ion manipulation in Penning traps, precise mass measurements, and selective $\beta$- and $\gamma$-decay studies has allowed for the first time the selection and study of isomerically pure samples from an ensemble of three different isomeric states of short-lived radioactive nuclei. A further exploration of these techniques, including post-acceleration of isomerically pure beams using schemes such as, e.g., REX-ISOLDE at ISOLDE [21], will create a large potential for reaction studies, of interest for nuclear structure and nuclear astrophysics investigations. Using these complementary techniques, the unambiguous identification and assignment of three $\beta$-decaying isomers in $^{70}$Cu has been accomplished and has led to corrected mass assignments for the three isomers as well as to further conclusions by comparisons with models for the structure of $^{70}$Cu and the $\beta$ decay of $^{70}$Ni. This is an important step towards understanding the complex nuclear structure of the exotic nuclides in the region of the $N = 40$ subshell closure. Mass measurement and nuclear spectroscopy results are in excellent agreement on the energy position of the $^{70}$Cu isomers. The calculations show that for the lowest multiplet the main component of the low-lying states is a $1\pi$-$1\nu$ configuration outside the closed $Z = 28$ shell and $N = 40$ subshell, but that a substantial neutron $2p$-$2h$ configuration contributes with at least 33%. This indicates a weak subshell closure at $N = 40$.

We acknowledge the LISOL and ISOLDE technical group for assistance during the experiments. N. A. S. thanks E. Caurier and F. Nowacki from IReS (Strasbourg) for useful discussions. This work was supported by the IUAP (P5/07), by the BMBF (06GF151), by the European Commission (IHRP HPRI-CT-1999-00018, IONCATCHER HPRI-CT-2001-50022, TARGISOL HPRI-CT-2001-50033, and NIPNET HPRI-CT-2001-50034), and by the FWO-Vlaanderen.

*Author to whom correspondence should be addressed. Electronic address: Klaus.Blaum@CERN.ch
†Present address: Department of Physics and Astronomy, University of Aarhus, Denmark.
‡Present address: NSCL, Michigan State University, East Lansing, 48824-1321 MI, USA.

[1] K. Langanke *et al.*, Phys. Rev. C **67**, 044314 (2003), and references therein.
[2] K. Langanke *et al.*, Phys. Rev. Lett. **90**, 241102 (2003).
[3] L. M. Taff *et al.*, Nucl. Phys. **A164**, 565 (1971).
[4] W. L. Reiter *et al.*, Nucl. Phys. **A249**, 166 (1975).
[5] E. Runte *et al.*, Nucl. Phys. **A399**, 163 (1983).
[6] R. Firestone, *Table of Isotopes* (Wiley, New York, 1996), 8th ed.
[7] J. D. Sherman *et al.*, Phys. Lett. **67B**, 275 (1977).
[8] G. Audi and A. H. Wapstra, Nucl. Phys. **A595**, 1 (1995); G. Audi *et al.*, Nucl. Phys. **A729**, 337 (2003).
[9] S. Franchoo *et al.*, Phys. Rev. C **64**, 054308 (2001).
[10] E. Kugler, Hyperfine Interact. **129**, 23 (2000).
[11] F. Herfurth *et al.*, J. Phys. B **36**, 931 (2003).
[12] L. Weissman *et al.*, Phys. Rev. C **65**, 024315 (2002).
[13] A. Kellerbauer *et al.*, Eur. Phys. J. D **22**, 53 (2003).
[14] J. Van Roosbroeck *et al.*, Phys. Rev. C (to be published); Ph.D. thesis, K.U. Leuven, 2002.
[15] M. H. Brennan *et al.*, Phys. Rev. **120**, 927 (1960).
[16] V. Paar *et al.*, Nucl. Phys. **A331**, 16 (1979).
[17] T. Ishii *et al.*, Phys. Rev. Lett. **81**, 4100 (1998).
[18] M. Hjorth-Jensen *et al.*, Phys. Rep. **261**, 125 (1995).
[19] F. Nowacki, Ph.D. thesis, IReS, Strasbourg, 1996.
[20] E. Caurier, shell-model code ANTOINE, IReS, Strasbourg, 1989–2002; E. Caurier and F. Nowacki, Acta Phys. Pol. **30**, 705 (1999).
[21] D. Habs *et al.*, Hyperfine Interact. **129**, 43 (2000).